ORGANELLE

RESEARCH OPEN ACCESS

Robust assembly of electron transfer chain in the brain of naked mole-rats during aging

Ting Liang,[1,#] Belinda Bernal,[1,#] Wenbo Qi,[2] Yuji Ikeno,[2,5,6] Adam B. Salmon,[2,4,6] Daisy Kwok,[3] Joel Michalek,[3] Mai Zhou,[7] and Yidong Bai[1,*]

[1]Department of Cell Systems and Anatomy
[2]Barshop Institute for Longevity and Aging Studies
[3]Department of Population Health Sciences, University of Texas Health San Antonio, San Antonio, TX 78229, USA
[4]Department of Molecular of Medicine, University of Texas Health San Antonio, San Antonio, TX 78229, USA
[5]Department of Pathology, University of Texas Health San Antonio, San Antonio, TX 78229
[6]Geriatric Research Education and Clinical Center, South Texas Veterans Healthcare System
[7]Department of Statistics, University of Kentucky, Lexington, KY 40536
*Correspondence: Dr. Yidong Bai, Email: baiy@uthscsa.edu
#These authors contributed equally.

ABSTRACT

Naked mole-rats (NMR, *Heterocephalus glaber*) are the longest-lived rodent species, with a maximum life span of more than 30 years. These long-lived mammals exhibit delayed aging phenotypes and resistance to age-related pathologies including neurodegeneration. Multiple regulatory pathways have been proposed for the anti-aging mechanisms in NMR including enhanced mitochondrial function and suppressed oxidative stress. In this study, we investigated the assembly of the electron transfer chain (ETC) which constitutes the structural base for the regulation of both oxidative phosphorylation and the production of reactive oxygen species (ROS), in brains from young and old NMR and C57BL/6 mice. While ETC assembly declined with aging in C57BL/6 mice, we found that NMR display a robust respiratory chain assembly at older ages in both males and females. Among them, individual complex IV and supercomplexes containing complex I and III or complex III and IV showed the most pronounced differences between two species. Our results indicate that a preserved robust assembly of ETC during aging contributes to enhanced mitochondrial oxidative phosphorylation and suppressed oxidative stress, which may contribute to the longevity and resistance to age-related pathologies in NMR.

Key words: Naked Mole-Rat (NMR); Aging; Mitochondrial Electron Transfer Chain; Blue Native Gel; Supercomplex

INTRODUCTION

Naked mole-rats (NMR; *Heterocephalus glaber*, Rodentia) are native to Eastern Africa and live in large subterranean colonies. One of this rodent species' most significant biological features is its extreme longevity, with a maximum life span of over 30 years in laboratory conditions [1]. In addition, this long-lived animal also exhibits a remarkably long health span with a relative lack of development of many age-related phenotypes seen in aging mice and rats including lordokyphosis, loss of fecundity, decreased thermoregulation capacities, elevated cardiac disorders, and muscle atrophy [2]. Moreover, they are able to preserve this good health despite living much longer than common laboratory rodents.

Multiple mechanisms have been proposed as the underlying drivers of longevity, delayed aging, and resistance to age-related diseases in NMR (Figure 1). Notably, many of the suggested "hallmarks" of aging seem to be differentially regulated in NMR compared to mice and rats, in ways generally supported as beneficial to aging. These include better-maintained genome stability and protein homeostasis, attenuated inflammation, regulation of senescence and death induction, and a relatively low accumulation of oxidative stress with age [3].

The regulation of mitochondrial function is a significant mechanism of aging and may serve as a central mediator of normal cellular function. Mitochondria are ubiquitous organelles found in all eukaryotic cells whose primary function is to generate energy through oxidative phosphorylation (OXPHOS) [4], though there is growing evidence for additional important homeostatic roles for mitochondria including the control of apoptosis [5], the modulation of calcium signals [6], and the regulation of cell proliferation [7]. During aging, mitochondrial function has been shown to decline in many ways including reduced bioenergetic functions, ineffective mitochondrial signaling, and increased generation of reactive oxygen species (ROS). The etiology of this mitochondrial dysfunction has been proposed to derive from many sources including the accumulation of mitochondrial DNA or protein damage, impaired biogenesis, and altered metabolic properties of mitochondrial enzymes. However, biophysical changes to mitochondria with age have been relatively less studied. High-energy electrons that prematurely leave the transfer chain generate reactive oxygen species (ROS), a primary

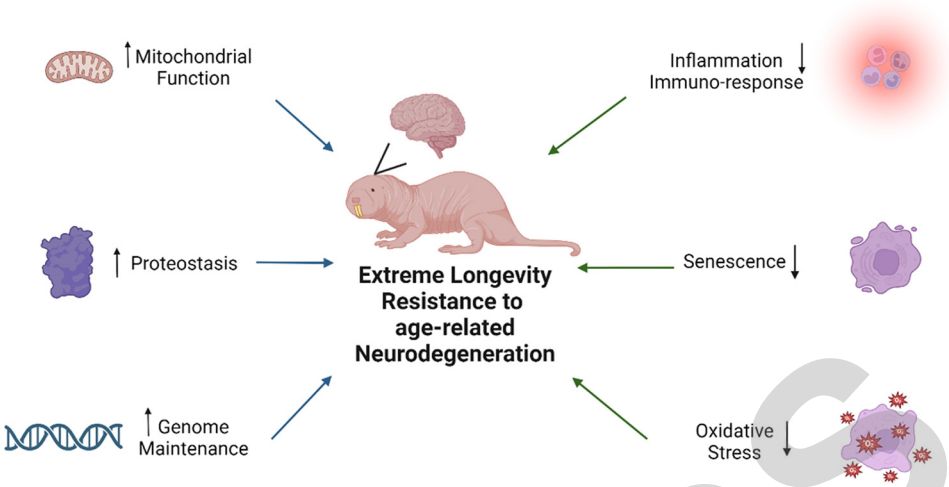

Figure 1. Potential factors contributing to longevity in naked mole rats
Created in BioRender. Bernal, B. (2023)

source of oxidative stress. ROS have long been thought of as toxic by-products of OXPHOS and are considered to be pathogenic agents for many diseases and aging [8]. More evidence has been generated suggesting that intracellular ROS also serve as important molecules in mediating both normal as well as pathological pathways [9].

OXPHOS is mediated by the mitochondrial respiratory chain (MRC) which is composed of five protein complexes including NADH-ubiquinone oxidoreductase (complex I), succinate-ubiquinone oxidoreductase (complex II), ubiquinone-cytochrome *c* oxidoreductase (complex III), and cytochrome *c* oxidase (complex IV); which are responsible for electron transfer; and ATP synthase as complex V. It is also interesting to note that the MRC functions not as isolated protein complexes floating in the inner mitochondrial membrane, but rather as organized multicomplex structures called supercomplexes (SC). The dynamics of organization and distribution of various forms of supercomplexes have been associated with the regulation of metabolism; however, maintenance and regulation of the respiratory chain structure in aging and human health have not been illustrated [10].

In this study, we conducted an exploratory investigation on the dynamics of respiratory chain assembly during aging to shed light on the potential role of energy metabolism and oxidative stress in the longevity and related phenotypes associated with naked mole-rats.

RESULTS

Identification of the mitochondrial respiratory chain in NMR

In this study, we compared samples from the NMR to that of C57BL/6 mice to compare the assembly of the mitochondrial electron transport chain (ETC) and its maintenance in a species of successful aging (NMR) vs normal aging (mice). The ETC maintains crucial processes of energy generation and cellular respiration that occur in the inner mitochondrial membrane. The assembly of the ETC involves the coordinated protein synthesis of genes encoded by both nuclear and mitochondrial genomes; import of various ETC complexes, subunits, and assembly factors; and subsequent assembly of individual and respiratory SC which contain multiple complexes (Figure 2). The assembly of the ETC provides a structural base for the coupling of electron transfer regulation of electron leakage, and maintenance of membrane potential for ATP production.

The robust assembly of the overall electron transfer complexes of old NMR in both males and females

To determine if the assembly of the ETC could provide a potential mechanism for longevity in NMR, we utilized Blue Native Gel Electrophoresis (BN-PAGE) technology which allows us to separate protein complexes based on their size and charge under native conditions, preserving their native structure and interactions, to analyze the ETC assembly during aging in both NMR and a common rodent model for aging research, C57BL/6 mice. After electrophoresis, the ETC complexes were then determined by western blot with antibodies against representative subunits of complex I, III, and IV (Figure 3). As sex is an important biological variant, we compared the BN-PAGE pattern of ETC complexes in young and old NMR and C57BL/6 mice in both females (Figure 3A) and males (Figure 3B).

We first compared the overall assembly of three individual ETC complexes which constitute the majority of electrons from the TCA cycle to the OXPHOS system in the form of NADH. While all three complexes exhibited decreased assembly in old compared with young in both female and male mice, NMR showed enhanced assemblies compared to mice in general and an increase in assembly in old samples versus young samples (Figure 4). That is, assembly declined with age in mice and increased with age in the NMR. Interestingly, among these ETC complexes, the terminal complex or complex IV showed the most significant cross-species difference with p-values at 1.93e-09 and 5.39e-10, in females and males, respectively.

The dynamics of assembly of respiratory complex I during aging

Complex I or NADH:ubiquinone oxidoreductase, is the largest and first enzyme complex in the mitochondrial electron transport chain (ETC). The assembly of complex I proceeds through the formation of intermediate subcomplexes, which involves the stepwise association of different subunits and assembly factors to form several modules, then further assembly into supercomplexes with complex III and IV.

Among all the complex I-containing respiratory complexes, we found that in female mice, individual complex I and the supercomplex containing complex I and III (SC I+III) showed a significant decrease in assembly during aging (Figure 5A). In NMR,

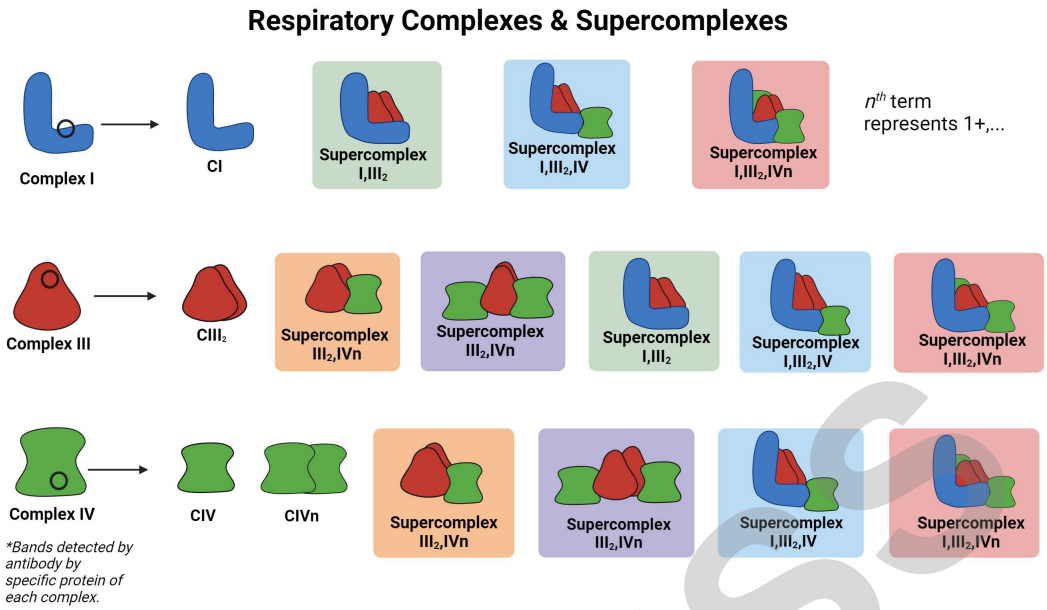

Figure 2. Respiratory chain assembly

Descriptive figure of the respiratory complex subunits and the potential supercomplex assemblies resulting from complex interaction. Created in BioRender. Bernal, B. (2023)

however, all respiratory complex assemblies including complex I, including the supercomplex with all three complexes (SC I+III+IV), increased significantly with age. In male mice and female NMR, SC I+III+IV increased somewhat and all complex I-containing respiratory complexes exhibited increased assembly during aging. Among these complexes, the individual complex I and SC I+III showed the largest cross-species difference with p-values of 2.46e-07 and 2.00e-07 (Figure 5A), in females and 7.60e-08 and 3.29e-07 in males, respectively.

The dynamics of assembly of respiratory complex III during aging

Mitochondrial complex III, also known as the bc1 complex or ubiquinol-cytochrome *c* oxidoreductase, sits in the middle of ETC. Accordingly, complex III is often found assembled into supercomplexes with other ETC complexes, primarily complex I and complex IV. It has been reported that there is no supercomplex III and IV (SC III+IV) assembly in C57BL/6 mice due to a genetic change [11].

We found that individual complex III assembly decreased in both female and male mice with age (Figure 6A, B). In NMR, SC III+IV showed the most increase in females and greater enhancement in males during aging. Interestingly, supercomplex III_2, IV_n showed dramatically higher levels of assembly in NMR compared to mice.

The dynamics of assembly of respiratory complex IV during aging

Complex IV or cytochrome *c* oxidase (COX), is the terminal enzyme complex of the ETC. As discussed before, complex IV can be found assembled into supercomplexes with complex I and III, respectively, or together.

We found that while individual complex IV assembly decreased in both female and male C57BL/6 mice during aging, all respiratory complexes involving complex IV increased in old NMR females and males.

The assembly of supercomplexes in aging

One of the most interesting findings of our study is the enhanced respiratory supercomplex assembly during NMR aging, while the opposite was recorded with C57BL/6 mice. We then further analyzed the assembly of each supercomplex detected by each component in both females and males.

As shown in Figure 8A, SC I+III exhibited consistent differences between NMR and C57BL/6 mice in both female and males. While such assembly decreased during aging in C57BL/6 mice, they increased significantly with NMR. Similarly, SC III+IV was increased in NMR during aging (Figure 8B). However, with supercomplexes containing complexes I, III, and IV, it seems the assembly of such complete respirasomes increased in both C57BL/6 mice and NMR. Nevertheless, the increase of assembly during aging is still very much evident in NMR in both females and males by any comparison (Figure 8C).

DISCUSSION

The similarities between humans and mice in gene function, biochemistry, bioenergetics, and physiology position mice as a most common mammalian model to investigate disease pathogenesis. However, there are large differences between the sizes and lifespans of humans and mice. Because humans are much larger than mice, there is a hindrance in the ability for the species to adapt to changes in the environment. Mice have a higher basal metabolic rate, seven times that of humans, causing a weak capability to maintain cellular homeostasis. Having a lower metabolic rate, humans have a greater ability to maintain cellular homeostasis, which contributes to a slower rate of aging [12]. Naked mole-rats are labeled as a naturally long-lived species. Although NMR and mice are both rodents with similar body sizes, NMR exhibit delayed aging phenotypes and resistance to age-related pathologies including neurodegeneration in a way that is similar to humans [13]. Thus, they could serve as a better model to study human aging and resistance to age-related human degenerative diseases.

The assembly of the mitochondrial oxidative phosphorylation machinery or respiratory chain is crucial for cellular energy

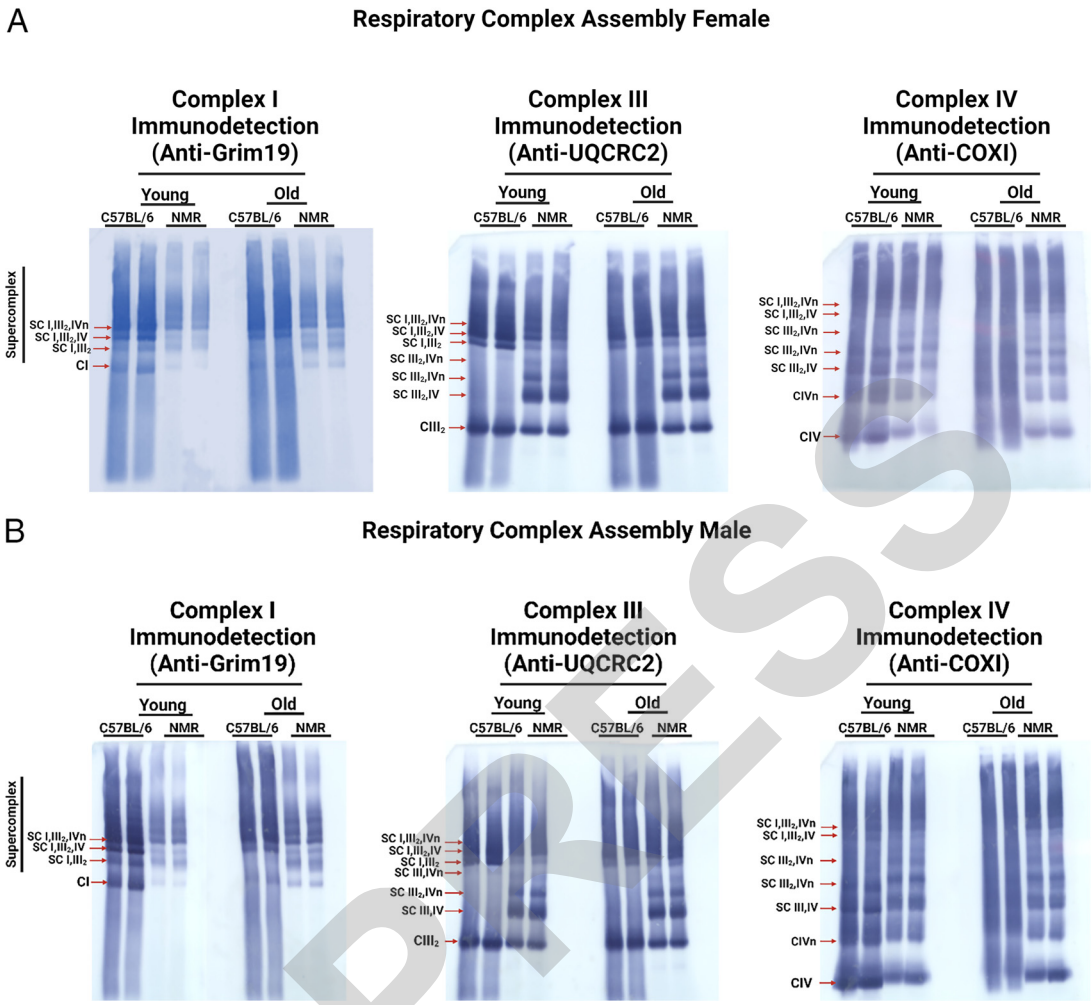

Figure 3. Electrophoretic analysis of BN-PAGE respiratory complex I, III, & IV by immunodetection

A) Immunoblot patterns of aging female C57BL/6 mice and naked mole-rats. **B)** Immunoblot patterns of aging male C57BL/6 mice and naked mole-rats. Created in BioRender. Bernal, B. (2023)

production and overall mitochondrial function. The proper assembly of the respiratory chain ensures efficient electron transfer, which will in turn drive the establishment of the proton gradient across the mitochondrial inner membrane, which is the basis of mitochondrial membrane potential. This potential is essential for maintaining mitochondrial integrity, various ion homeostases, and processes like mitochondrial dynamics and mitophagy. While the mitochondrial respiratory chain plays a vital role in ATP production, it is also a primary source of reactive oxygen species (ROS), especially when a disruption in the electron flow causes leakage. Thus, the proper assembly of the respiratory chain can not only facilitate energy production but also suppress ROS production and reduce oxidative stress which could directly damage the cellular components irreversibly and contribute to aging and age-related pathological phenotypes.

Our studies highlighted the enhanced overall respiratory chain assembly in NMR during aging. Comparatively, we found that the assemblies of individual complex IV, SC I+III, and SC III+IV exhibited the most pronounced enhancement. Complex IV, or cytochrome *c* oxidase, is the terminal complex in the electron transport chain. Complex IV is comprised of 13 polypeptide subunits, three of which are encoded in the mitochondrial genome [14]. COX reduces oxygen molecules to a water molecule and provides hydrogens to the intermembrane space to generate membrane potential for ATP production. The electron transfer at complex IV involves cytochrome c, copper centers, and iron-containing heme groups. Complex IV also has the guiding effect of stabilizing and managing the maturation of ETC complexes [11].

During the process of electron transport, a small percentage of electrons leaking from complexes I and III can react with molecular oxygen to form superoxide radicals ($O_2^{\bullet -}$), which are the primary ROS generated within mitochondria. Increased assembly of supercomplex I and III would thus increase the efficiency of electron transfer and decrease the susceptibility to oxidative stress. Similarly, the association of complex III and IV leads to a decrease in the intercomplex distance. The shorter diffusion distance via the water phase of the intermembrane space would result in a higher oxidoreductase activity. It is also noted that the cytochrome c-mediated electron transfer has been suggested as rate limiting [15].

Our investigation provided a surprising yet promising framework to explain the NMR's fascinating longevity and resistance to age-related pathology. We want to acknowledge that the further validation of the significance of respiratory chain assembly depends on the

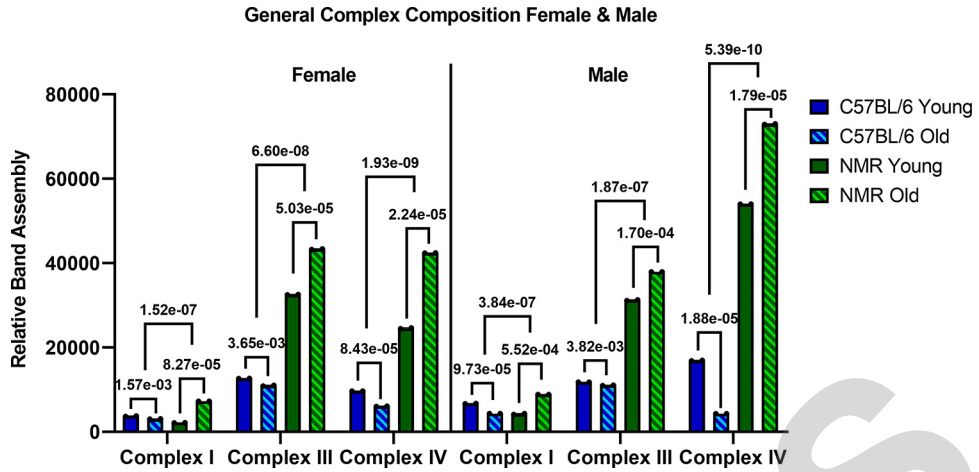

Figure 4. Quantitative analysis of BNG respiratory complex I, III, & IV

A one-way ANOVA was used to obtain p-value 1 (C57BL/6 young vs. old) & p-value 2 (NMR young vs. old) within species young-old interaction term, n = 2. Two-way ANOVA was used to obtain p-value 3, cross specie young-old interaction term, n = 4. Complex I is the detection of all the bands identified with the complex I BN-PAGE immunodetection using Anti-Grim19 antibody. Complex III is the detection of all bands identified with the complex III BN-PAGE immunodetection using Anti-UQCRC2 antibody. Complex IV is the detection of all bands identified with the complex IV BN-PAGE immunodetection using Anti-COXI antibody.

investigation of the implications of biological function and details of the molecular mechanism. We certainly anticipate that further characterization of the respiratory chain assembly process would provide a unique opportunity to understand the regulation of energy and oxidative metabolisms which could lead to breakthroughs in combating aging and age-related diseases.

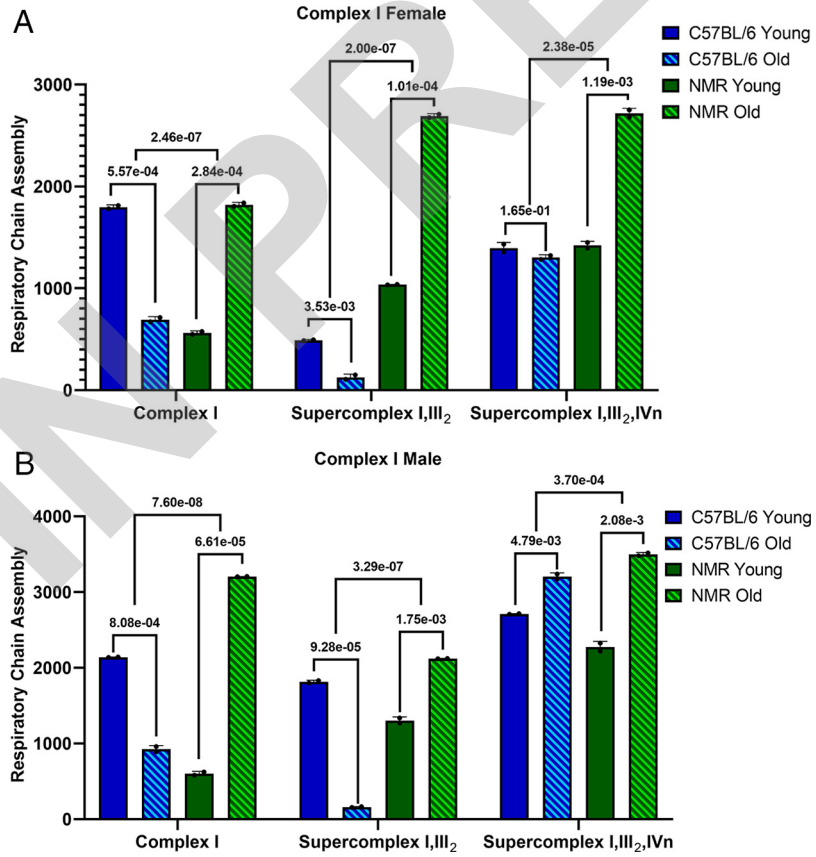

Figure 5. Quantitative analysis of BNG respiratory complex I & complex I-containing supercomplexes

A one-way ANOVA was used to obtain p-value 1 (C57BL/6 young vs. old) & p-value 2 (NMR young vs. old) within species young-old interaction term, n = 2. Two-way ANOVA was used to obtain p-value 3, cross specie young-old interaction term, n = 4. **A)** C57BL/6 & NMR Females. **B)** C57BL/6 & NMR Males. In the BN-PAGE for Complex I, the three types of bands detected and identified as 'Complex I', 'Supercomplex I, III_2', and 'Supercomplex I, III_2, IVn'. **(A)** & **(B)** Complex I band was detected by the antibody Anti-Grimm19. Supercomplex I, III_2 band was identified by both antibodies, Anti-Grimm19 and Anti-UQCRC2. Supercomplex I, III_2, IVn bands were identified by three antibodies, Anti-Grimm19, Anti-UQCRCR2 and Anti-COXI. 'n' in Supercomplex I, III_2, IVn means the sum of multiple bands identified by the antibodies containing varying numbers of complex IV.

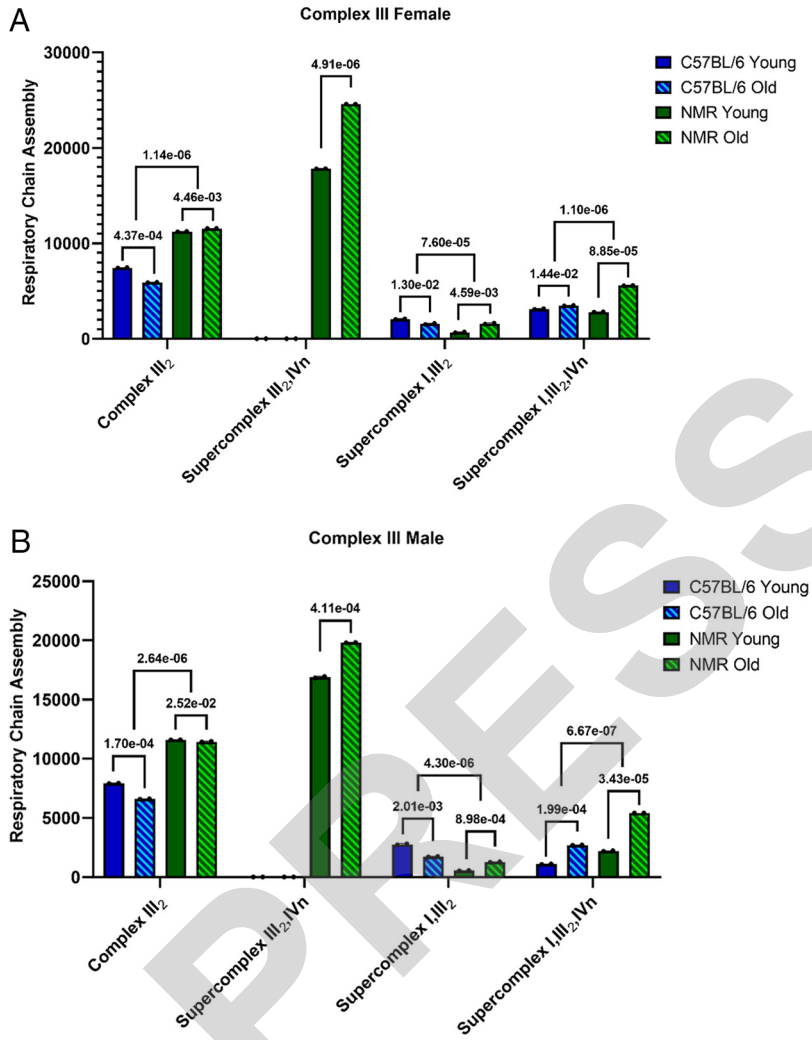

Figure 6. Quantitative analysis of BNG respiratory complex III & complex III-containing supercomplexes

A one-way ANOVA was used to obtain p-value 1 (C57BL/6 young vs. old) & p-value 2 (NMR young vs. old) within species young-old interaction term, n = 2. Two-way ANOVA was used to obtain p-value 3, cross specie young-old interaction term, n = 4. **A)** C57BL/6 & NMR Females. **B)** C57BL/6 & NMR Males. In the BN-PAGE for complex III, the four types of bands detected and identified were 'Complex III_2', 'Supercomplex III_2, IVn', 'Supercomplex I, III_2,' and 'Supercomplex I, III_2, IVn'. Complex III is more interactive in its dimer form, explaining the subscript '2' in the figure. **(A)** & **(B)** Complex III_2 band was identified with antibody, Anti-UQCRC2. Supercomplex III_2, IVn was identified with antibodies Anti-UQCRC2 and Anti-COXI only in NMR.'n' in Supercomplex III_2, IVn means the sum of multiple bands identified by antibody, Anti-COXI, containing varying numbers of complex IV. As explained previously, C57BL/6 does not produce Supercomplex III_2, IVn, these bands were not detected by the antibodies in C57BL/6. Supercomplex I, III_2, IVn was identified by antibodies Anti-Grim19, Anti-UQCRC2, and Anti-COXI. 'n' in Supercomplex I, III_2, IVn means the sum of multiple bands identified by the antibodies containing varying numbers of complex IV.

MATERIALS AND METHODS

Animal preparation

C57BL/6 mice were purchased from Jackson Lab and were aged 6 and 26 months at the UTHSCSA animal facility. Naked mole-rat were born in a laboratory breeding colony at the Barshop Institute, UT Health San Antonio. Naked mole-rat were housed under semi-natural conditions in an artificial burrow system within a colony room under normoxia. The young males were 2.77 years old, and young females were 2.77 and 4.57 years old. The older males were 32.70 years old and the older females were 15.38 and 15.94 years old.

Experimental procedures on mice and naked mole-rat were approved by the UTHSCSA Institutional Animal Care and Use Committee, following the National Institutes of Health guidelines.

Mitochondrial preparation and electrophoresis of respiratory complexes

Mitochondria were isolated according to procedures described previously [16]. Mitochondrial protein concentration was measured using the Bradford method. Blue-native PAGE (BN-PAGE) was used for the separation of respiratory complexes on a 4-13% gradient polyacrylamide gel. About 50 µg of mitochondrial proteins were loaded according to procedures described previously [16]. The protein complexes were detected by western blot with the following antibodies (Mitosciences); MS111 against NDUFA9 of complex I and MS304 against core 2 of complex III [17]. The western blot was carried out according to the protocol provided by Mitosciences. In parallel, the same amount of protein was loaded on an SDS polyacrylamide gel and immunoblotted with antibody MSA03 against porin (VDAC), which was used as a loading control.

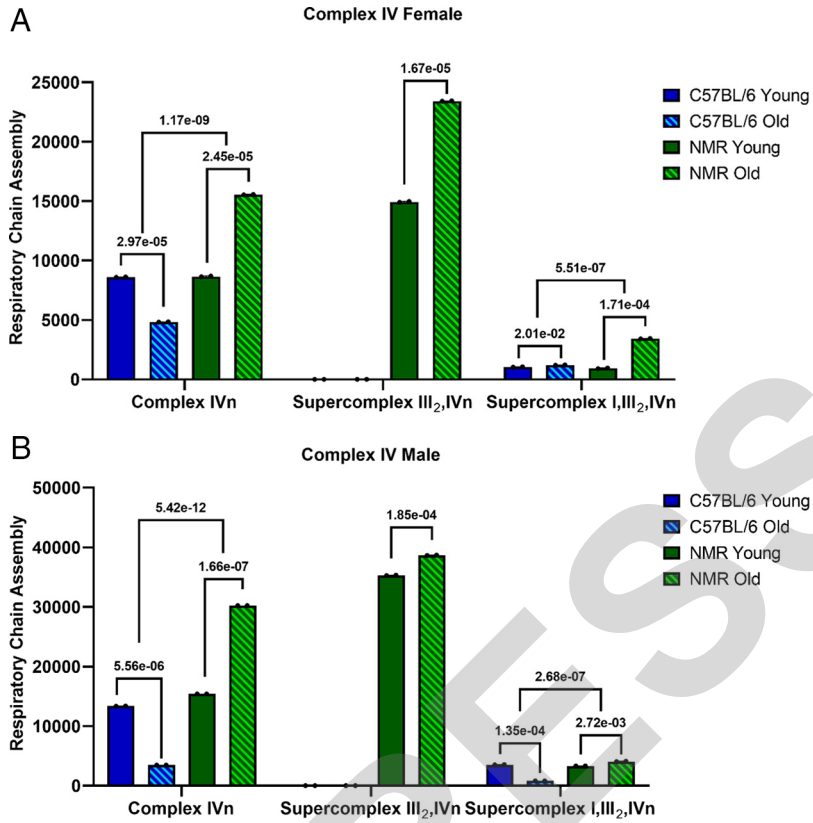

Figure 7. Quantitative analysis of BNG respiratory complex IV & complex IV-containing supercomplexes

A one-way ANOVA was used to obtain p-value 1 (C57BL/6 young vs. old) & p-value 2 (NMR young vs. old) within species young-old interaction term, n = 2. Two-way ANOVA was used to obtain p-value 3, cross specie young-old interaction term, n = 4. **A)** C57BL/6 & NMR Females. **B)** C57BL/6 & NMR Males. In the BN-PAGE for complex IVn, the three types of bands detected and identified were 'Complex IVn', 'Supercomplex III_2, IVn', and 'Supercomplex I, III_2, IVn'. **(A)** & **(B)** Complex IVn, 'n' meaning the sum of the multiple bands identified by the antibody, Anti-COXI. Supercomplex III_2, IVn was identified by antibodies Anti-UQCRC2 and Anti-COXI. 'n' in Supercomplex III_2, IVn means the sum of multiple bands identified by antibody, Anti-COXI, containing different varieties of numbers of complex IV. As explained previously, C57BL/6 does not produce supercomplex III_2, IVn, these bands were not detected by the antibodies in C57BL/6. Supercomplex I, III_2, IVn was identified by antibodies Anti-Grim19, Anti-UQCRC2, and Anti-COXI. 'n' in supercomplex I, III_2, IVn means the sum of multiple bands identified by the antibodies containing varying numbers of complex IV.

Gel imaging processing: A quantitative analysis was conducted on the blue native gels utilizing Fiji Image J (version 1.54f) to obtain the densitometry. For each image, the background was adjusted to accurately calculate the densitometry. For Complex I Female BNG, the background subtraction rolling ball radius was adjusted to 800 pixels light. The Complex III Female background was first sharpened then the rolling ball radius was adjusted to 800 pixels light background afterwards being adjusted once again. For Complex IV Female BNG, the background rolling ball radius was adjusted to 800 pixels light background then sharpened twice, smoothed, adjusted pixels to 1000, and sharpened once again. The adjustment to the blue native gels for the males was similar to the females. For Complex I Male, the BNG was first sharpened twice then the background rolling ball radius was adjusted to 800 pixels. The Complex III Male BNG was adjusted to 800 pixels then sharpened twice followed by smoothed. Lastly, Complex IV Male was adjusted to 800 pixels rolling ball radius then changed to 1000 pixels followed by sharpened twice. Each blue-native gel was analyzed with preciseness and proficiency to eliminate errors and miscalculations. The acquired data was stored in Google Sheets and Microsoft Excel. Using both programs, the data was cleaned and organized, then transferred to GraphPad Prism (version 8.42 679) to create the figures.

Statistical analysis: The statistical analysis was performed using R Studio (version 2023.12.0 + 369) and Microsoft Excel (version 18.2311.1071.0). Once all graphs were created, codes were created to calculate the p-values for the data using one-way and two-way ANOVA. The statistical analysis was conducted on the basis of four factors: species, sex, age, and complex. Each factor is broken down into the following: specie, C57BL/6 (n ¼ 4) and NMR (n ¼ 4); sex, female (n ¼ 2) and male (n ¼ 2); age, young and old; and complex, I, III, and IV. To further group the factors, the species are each analyzed by sex (female and male) and age (young and old), with respect to the individual respiratory complexes. The respiratory supercomplexes are unique to the individual complex as seen in Figure 2. Figures 5-8 display the analysis between the different factors for each specie in age, sex, and complex. There are a total of three p-values on the figures. In Figures 3-7 A/B, p-values 1 and 2 were obtained by a one-way ANOVA test with n = 2 for each specie-sex specific group. These p-values identify the significance within each specie group based on age. P-value 3 was obtained using a two-way ANOVA test to calculate the difference of the difference between each species and age group, n = 4. In addition, the percentage of change was also calculated to identify how much the groups increased or decreased with age. Further, to create a more

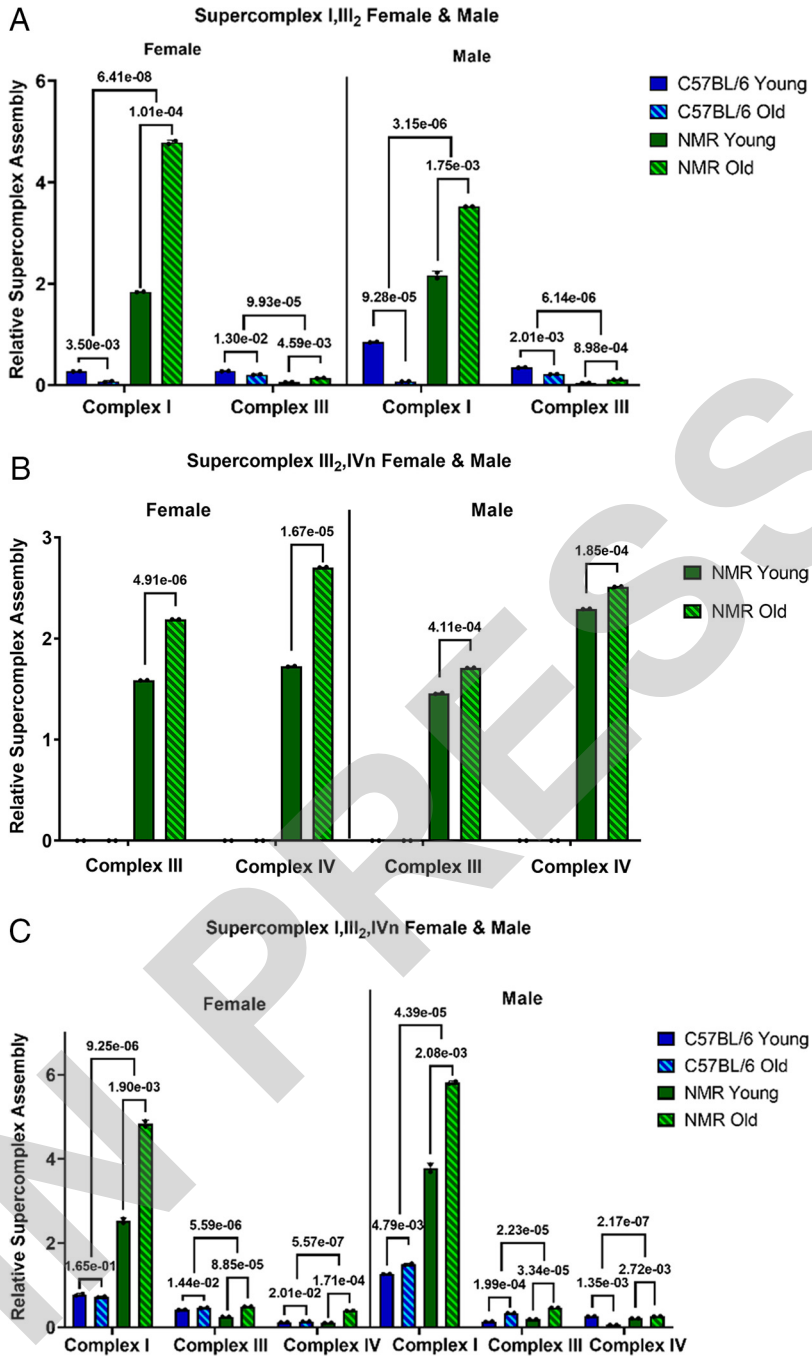

Figure 8. Quantitative analysis of BNG complex subunit detection of supercomplex by antibody

A one-way ANOVA was used to obtain p-value 1 (C57BL/6 young vs. old) & p-value 2 (NMR young vs. old) within species young-old interaction term, n = 2. Two-way ANOVA was used to obtain p-value 3, cross specie young-old interaction term, n = 4. **A)** Supercomplex I, III_2 C57BL/6 & NMR Females & Males. Supercomplex I, III_2 was detected by antibodies Anti-Grim19 and Anti-UQCRC2. Complex I represents the detection by antibody, Anti-Grim19. Complex III represents the detection by Anti-UQCRC2. **B)** Supercomplex III_2, IVn C57BL/6 & NMR Females & Males. Supercomplex III_2, IVn was detected by antibodies Anti- UQCRC2 and Anti-COXI. Complex III represents the detection by antibody Anti-UQCRC2. Complex IV represents the detection of Anti-COXI. Supercomplex III_2, IVn was not detected by antibodies in C57BL/6 mice. **C)** Supercomplex I, III_2, IVn C57BL/6 & NMR Females & Males. Supercomplex I, III_2, IVn was detected by antibodies Anti-Grim19, Anti-UQCRC2 and Anti-COXI. Complex I represents the detection by Anti-Grim19. Complex III represents the detection by Anti-UQCRC2. Complex IV represents the detection by Anti-COXI.

extensive analysis of the supercomplex detection in each complex subunit, the data was normalized to one versus the change, increase or decrease. Each individual complex subunit was normalized to one with the supercomplexes normalized to their respective complex subunit. Figures 8 A-C portray the results of the normalization and the difference between aging C57BL/6 and NMR. P-values 1, 2, and 3 were calculated the same as for Figures 3-7. These graphs display the sex comparison of the detection of supercomplex by each individual complex subunit once the data has been normalized to each complex subunit.

ACKNOWLEDGMENTS

We would like to thank Drs. Rochelle Buffenstein, James Nelson, and Habil Zare for their helpful discussion. Zhenbo Zhang and Sammy Pardo for helping with image processing.

FUNDING

This work is supported by grants from the Baptist Health Foundation of San Antonio (YB), NIH R01CA283840 (YB), R01AG070034 (YI), and P30AG044271. NMR resources were supported by the San Antonio Nathan Shock Center Animal Core NIH P30 AG AG013319 [18].

CONFLICT OF INTEREST

The authors have no conflict of interest to report.

DATASETS/DATA AVAILABILITY STATEMENT

The data associated with this study is openly available upon request.

REFERENCES

1. Edrey, Y. H., Hanes, M., Pinto, M., Mele, J., & Buffenstein, R. (2011). Successful aging and sustained good health in the naked mole rat: a long-lived mammalian model for biogerontology and biomedical research. *ILAR journal*, *52*(1), 41–53. doi:10.1093/ilar.52.1.41.
2. Munro, D., Baldy, C., Pamenter, M. E., & Treberg, J. R. (2019). The exceptional longevity of the naked mole-rat may be explained by mitochondrial antioxidant defenses. *Aging cell*, *18*(3), e12916. doi:10.1111/acel.12916.
3. Maldonado, E., Morales-Pison, S., Urbina, F., & Solari, A. (2023). Aging Hallmarks and the Role of Oxidative Stress. *Antioxidants (Basel, Switzerland)*, *12* (3), 651. doi:10.3390/antiox12030651.
4. Sharma, L. K., Lu, J., & Bai, Y. (2009). Mitochondrial respiratory complex I: structure, function and implication in human diseases. *Current medicinal chemistry*, *16* (10), 1266–1277. doi:10.2174/092986709787846578.
5. Wang X. (2001). The expanding role of mitochondria in apoptosis. *Genes & development*, *15*(22), 2922–2933.
6. Falcke, M., Hudson, J. L., Camacho, P., & Lechleiter, J. D. (1999). Impact of mitochondrial Ca2 + cycling on pattern formation and stability. *Biophysical journal*, *77*(1), 37–44. doi:10.1016/S0006-3495(99)76870-0.
7. Rustin P. (2002). Mitochondria, from cell death to proliferation. *Nature genetics*, *30*(4), 352–353. doi:10.1038/ng0402-352.
8. Checa, J., & Aran, J. M. (2020). Reactive Oxygen Species: Drivers of Physiological and Pathological Processes. *Journal of in˜ammation research*, *13*, 1057–1073. doi:10.2147/JIR.S275595.
9. Lenaz G. (2001). The mitochondrial production of reactive oxygen species: mechanisms and implications in human pathology. *IUBMB life*, *52*(3–5), 159–164. doi:10.1080/15216540152845957.
10. Novack, G. V., Galeano, P., Castaño, E. M., & Morelli, L. (2020). Mitochondrial Supercomplexes: Physiological Organization and Dysregulation in Age-Related Neurodegenerative Disorders. *Frontiers in endocrinology*, *11*, 600. doi:10.3389/fendo.2020.00600.
11. Yu, C., Li, Y., Holmes, A., Szafranski, K., Faulkes, C. G., Coen, C. W., Buffenstein, R., Platzer, M., de Magalhães, J. P., & Church, G. M. (2011). RNA sequencing reveals differential expression of mitochondrial and oxidation reduction genes in the long-lived naked mole-rat when compared to mice. *PloS one*, *6* (11), e26729. doi:10.1371/journal.pone.0026729.
12. Demetrius, L., *Of mice and men. When it comes to studying ageing and the means to slow it down, mice are not just small humans. EMBO Rep*, 2005. *6 Spec No* (Suppl 1): p. S39–44. doi:10.1038/sj.embor.7400422.
13. Lewis, K. N., Soifer, I., Melamud, E., Roy, M., McIsaac, R. S., Hibbs, M., & Buffenstein, R. (2016). Unraveling the message: insights into comparative genomics of the naked mole-rat. *Mammalian genome: of˚cial journal of the International Mammalian Genome Society*, *27*(7–8), 259–278. doi:10.1007/s00335-016-9648-5.
14. Vercellino, I., & Sazanov, L. A. (2022). The assembly, regulation and function of the mitochondrial respiratory chain. *Nature reviews Molecular cell biology*, *23*(2), 141–161. doi:10.1038/s41580-021-00415-0.
15. Brzezinski, P., Moe, A., & Ädelroth, P. (2021). Structure and Mechanism of Respiratory III-IV Supercomplexes in Bioenergetic Membranes. *Chemical reviews*, *121*(15), 9644–9673. doi:10.1021/acs.chemrev.1c00140.
16. Liang, T., Deng, J., Nayak, B., Zou, X., Ikeno, Y., & Bai, Y. (2022). Characterizing the Electron Transport Chain: Structural Approach. *Methods in molecular biology (Clifton, N.J.)*, *2497*, 107–115.
17. Li, H., Shen, L., Hu, P., Huang, R., Cao, Y., Deng, J., Yuan, W., Liu, D., Yang, J., Gu, H., & Bai, Y. (2017). Aging-associated mitochondrial DNA mutations alter oxidative phosphorylation machinery and cause mitochondrial dysfunctions. *Biochimica et biophysica acta Molecular basis of disease*, *1863*(9), 2266–2273. doi:10.1016/j.bbadis.2017.05.022.
18. Salmon, A. B., Nelson, J. F., Gelfond, J. A. L., Javors, M., Ginsburg, B., Lopez-Cruzan, M., Galvan, V., Fernandez, E., Musi, N., Ikeno, Y., Hubbard, G., Lechleiter, J., Hornsby, P. J., & Strong, R. (2021). San Antonio Nathan Shock Center: your one-stop shop for aging research. *GeroScience*, *43*(5), 2105–2118. doi:10.1007/s11357-021-00417-y.